

Microvessel density of malignant and benign hepatic lesions and MRI evaluation

Jian-Ping Lu, Jian Wang, Tao Wang, Yi Wang, Wei-Qing Wu, Li Gao

Jian-Ping Lu, Jian Wang, Department of Radiology, Changhai Hospital, Second Military Medical University, Shanghai 200433, China

Tao Wang, Yi Wang, Wei-Qing Wu, Eastern Hepatobiliary Surgery Institute, Second Military Medical University, Shanghai 200433, China

Li Gao, Department of Pathology, Changhai Hospital, Second Military Medical University, Shanghai 200433, China

Supported by the National Natural Science Foundation of China, No. 39970728

Correspondence to: Dr. Jian-Ping Lu, Department of Radiology, Changhai Hospital, Second Military Medical University, Shanghai 200433, China

Telephone: +86-21-25072133

Received: 2003-08-23 **Accepted:** 2003-10-12

Abstract

AIM: To study the difference of microvessel density (MVD) between malignant and benign hepatic lesions and study the relationship between MVD and dynamic enhanced magnetic resonance imaging (MRI) for evaluation of microvessels within malignant and benign hepatic lesions.

METHODS: A total of 265 specimens of hepatocellular carcinoma (HCC), 122 cirrhosis tissues and 22 hepatic benign lesions were enrolled for MVD by immunohistochemistry on tissue microarray, of which 49 underwent MRI examination before surgery, then contrast-to-noise ratios (CNR) and enhancement index (EI) in all the phases were calculated. Pearson correlation was performed for correlation analysis between CNR, EI and MVD.

RESULTS: MVD of HCC was 22.7 ± 15.8 (mean \pm SD), which was obviously higher than that of cirrhosis tissue (8.3 ± 7.6 , $P < 0.01$), but was not statistically different from that of benign lesions (31.3 ± 22.7 , $P > 0.05$). Among HCC, MVD of grades I-II was 29.9 ± 18.6 , which was much higher than those of grade III (22.2 ± 18.2 , $P < 0.01$) and grade IV (22.9 ± 19.0 , $P < 0.01$). MVD of HCC ($P = 0.018$) and of benign lesions ($P = 0.014$) were both correlative with CNR in arterial phase.

CONCLUSION: Neoangiogenesis is an important feature for malignant tumor, and MVD may act as a biological marker in differentiating malignant from benign hepatic lesions. Dynamic enhanced MRI, especially image in arterial phase, may act as an MVD evaluation criterion for malignant and benign hepatic lesions.

Lu JP, Wang J, Wang T, Wang Y, Wu WQ, Gao L. Microvessel density of malignant and benign hepatic lesions and MRI evaluation. *World J Gastroenterol* 2004; 10(12): 1730-1734
<http://www.wjgnet.com/1007-9327/10/1730.asp>

INTRODUCTION

It is well known that hepatocellular carcinoma (HCC) is a type of hypervascular lesion^[1], but there were seldom reports on

difference of microvessel density (MVD) between HCC and benign hepatic lesions. The tissue microarray, which has been developed recently as a high-throughput technique for rapid scanning hundreds or thousands of samples at the same time, can be applied in analyzing expression of some DNA, RNA or protein^[2]. In this research, differences of MVD of a large number of hepatic malignant and benign lesions were studied with tissue microarray, which further demonstrated some biological features of HCC.

Recent advances in magnetic resonance imaging (MRI) have led to the establishment of fast scan techniques, which, combined with bolus injection of contrast material, allows the acquisition of dynamic enhanced MRI for higher confident detection of HCC^[3-5]. There have been reports on correlation among digital subtraction angiography (DSA), ultrasound angiography (USAG), computed tomography during arterial portography (CTAP) and immunohistochemical findings^[6], but the relationship between MVD and dynamic MRI has been seldom reported. In this research, correlation between MVD and dynamic enhanced MRI of hepatic malignant and benign lesions was studied in order to establish a theoretical foundation for microvessels evaluation within these lesions with MRI images, which will give more references to clinical diagnosis or HCC therapy.

MATERIALS AND METHODS

Tissue specimens

Tissue specimens were obtained at surgery from Eastern Hepatobiliary Surgery Institute, including 265 of HCC, 122 of cirrhosis tissue adjacent to carcinoma, 5 of hepatocellular adenoma and 17 of focal nodular hyperplasia (FNH). The 265 specimens of HCC included 45 of small HCC (tumor diameter ≤ 3 cm). All the case of HCC were graded by Edmondson-Steiner's pathological criteria into 3 groups: grades I-II (37 cases), grade III (218 cases) and grade IV (10 cases). All the specimens were fixed in 10% formalin and embedded in paraffin. All the pathologic diagnoses were confirmed by two the pathologists.

Constructing tissue microarray

For tissue microarray construction, a hematoxylin and eosin (H&E)-stained section was made from each block to define representative regions. With a tissue-microarray-constructor (Beecher Instruments, Silver Spring, MD), a hole (diameter=6 mm) was punched into a recipient paraffin block, and then a cylindrical core sample (diameter=6 mm), which had been punched from the donor tissue block, was deposited into the hole. This process was repeated till all the samples were deposited into the recipient block. After finishing the recipient block, multiple sections were cut from the block with a microtome.

Immunohistochemical staining and evaluation criteria

Avidin-biotin-peroxidase complex (ABC) method was used for immunohistochemical staining with monoclonal antibody CD-34 (Antibody Dignostic Inc., U.S.A.). After staining, the tubular, sinusoidal, cystiform or vacuolar structures shaped by endothelial cells or immature endothelial cells, which were stained yellow

or brown by CD34, were considered as positive microvessels. In high power microscopic views, all the positive microvessels were counted for MVD.

MRI technique

Forty-eight patients with 49 of the lesions underwent MRI examination before surgery, including 33 HCC (only one belonged to grade IV, and the others belonged to grade III and all diameters were ≤ 3 cm) and 16 benign lesions. MRI was performed with a 1.5 T system (Symphony, Siemens) and a phased array coil was used. All the patients underwent axial T1 weighted (fast low angle shot, FLASH, TR=123 ms, TE=4.8 ms), T2 weighted (half-fourier acquisition single-shot turbo spin echo, HASTE, TR=1 200 ms, TE=57 ms) and multiphase dynamic gadolinium-DTPA enhanced (the same sequence as T1 weighted) imaging. The section thickness was 8 mm, with an intersection gap of 0.5-2 mm. The contrast material dose was 0.2 mmol/kg b.w. and was administered as a rapid bolus. Arterial phase images were obtained in 15-20 s after the start of bolus administration. Portal venous and equilibrium phase images were obtained in the 45 s and 90 s, respectively.

Image analyses

In all the images, signal intensities of lesions (SI_l), liver parenchyma (SI_p) and background noise (SI_n) were evaluated, respectively. Signal-to-noise ratios (SNR) of lesions and parenchyma were both calculated as $SNR = SI_l / SI_n$. Contrast-to-noise ratios (CNR) in all the phases were calculated as $CNR = SNR_l - SNR_p$. Enhancement indexes (EI) of lesions in all the phases were calculated as $EI = (SNR_{\text{contrasted}} - SNR_{\text{uncontrasted}}) / SNR_{\text{uncontrasted}}$.

Statistical analyses

All data were analyzed by SPSS 9.0. Analysis of variance was used to determine significant differences of MVD among HCC, cirrhosis and benign lesion, of MVD of HCC among different pathological grades and tumor diameters, and of CNR between HCC and benign lesion among nonenhanced, arterial, portal venous and equilibrium phases. Pearson correlation was performed for correlation analysis among CNRs, EIs and MVD in arterial, portal venous and equilibrium phases of HCC or

benign lesion, respectively.

RESULTS

Outcome of tissue microarray constructing, immunohistochemical staining and MRI

Overview of a piece of tissue microarray is shown in Figure 1. Microvessel density stained by immunohistochemistry and dynamic MR images of HCC, hepatocellular adenoma and FNH are shown in Figures 2, 3 and 4, respectively.

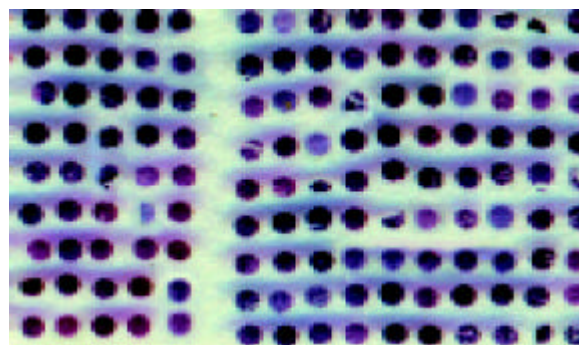


Figure 1 Overview of a piece of tissue microarray including 234 samples (HE staining).

Table 1 MVD of malignant and benign liver lesions

	Number	MVD (mean \pm SD)
HCC	265	22.7 \pm 15.8 ^b
Cirrhosis	122	8.3 \pm 7.6
Benign lesion	22	31.3 \pm 22.7

^b $P < 0.01$ vs cirrhosis.

MVD of hepatic benign and malignant lesions

MVD of HCC was significantly higher than that of cirrhosis, but there was no significant difference between those of HCC and of benign lesions (Table 1).

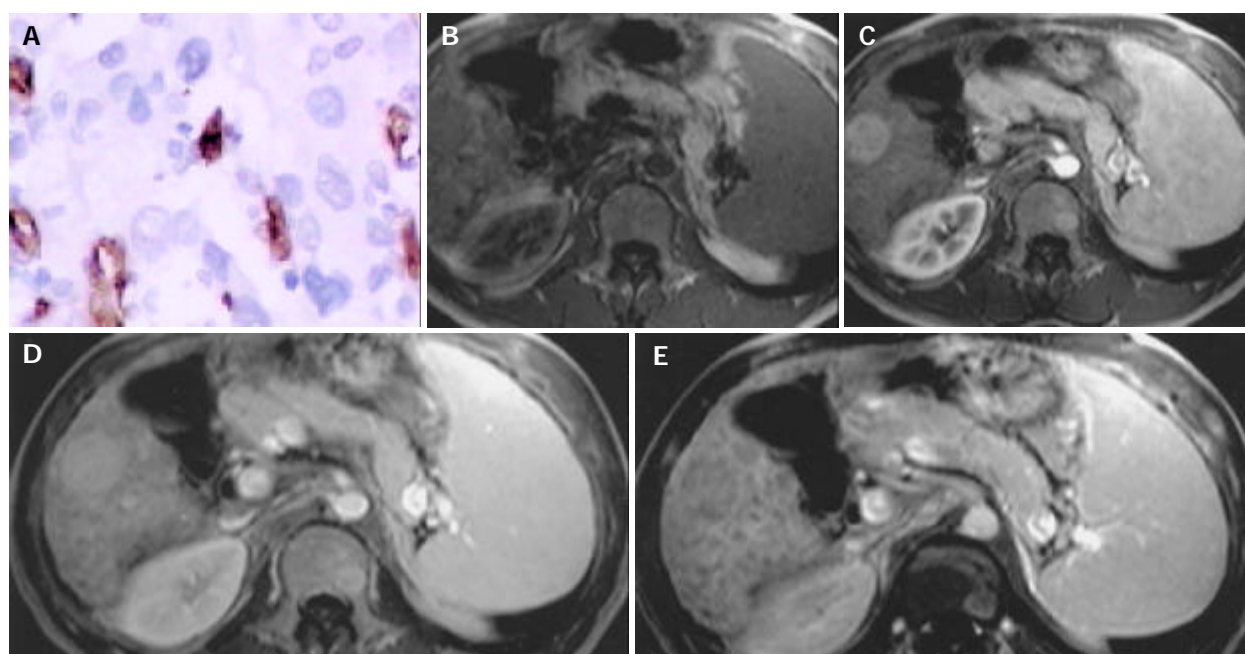


Figure 2 HCC in right lobar of liver. A: Microvessel density, stained by CD34 (Original magnification: $\times 200$); B: MR image, T1 weighted, nonenhanced, CNR=-1.50; C: MR image, arterial phase, CNR=11.00; D: MR image, portal venous phase, CNR=10.50; E: MR image, equilibrium phase, CNR=-6.00.

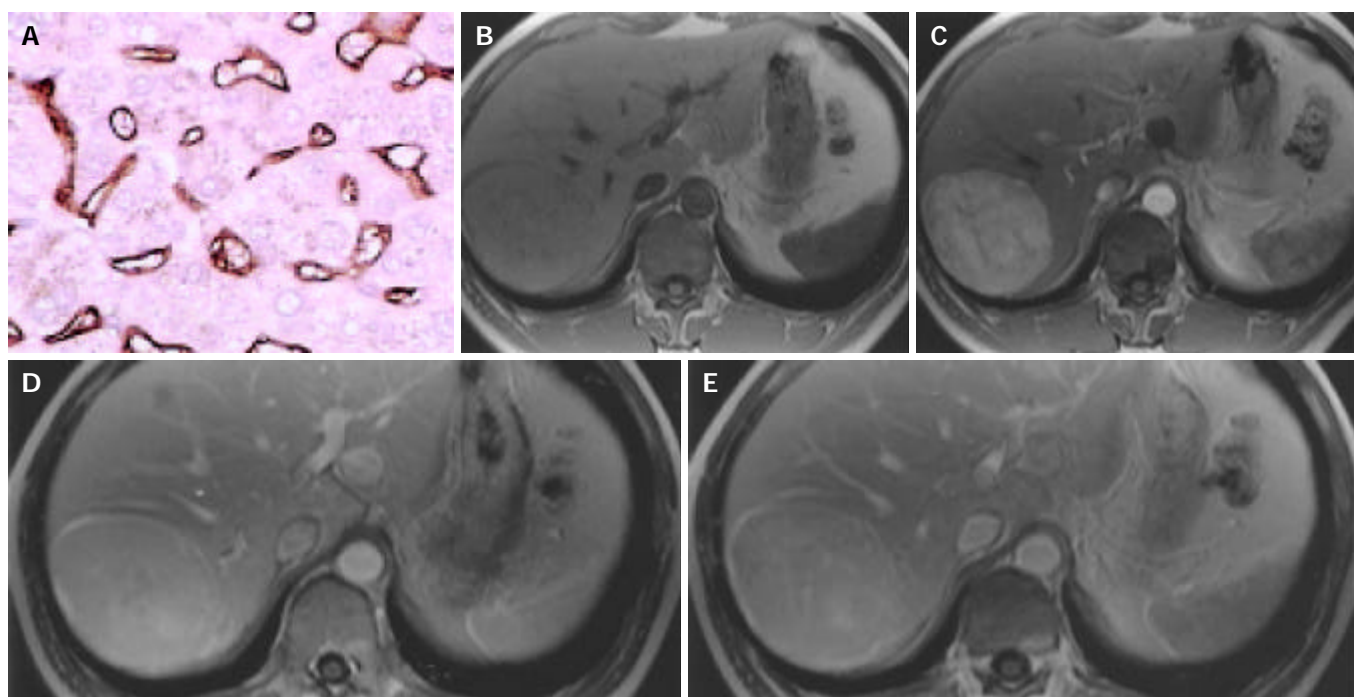


Figure 3 Hepatocellular adenoma in right lobar of liver. A: Microvessel density, stained by CD34 (Original magnification: $\times 200$); B: MR image, T1 weighted, nonenhanced, $CNR = -0.10$; C: MR image, arterial phase, $CNR = 16.93$; D: MR image, portal venous phase, $CNR = 9.42$; E: MR image, equilibrium phase, $CNR = 6.42$.

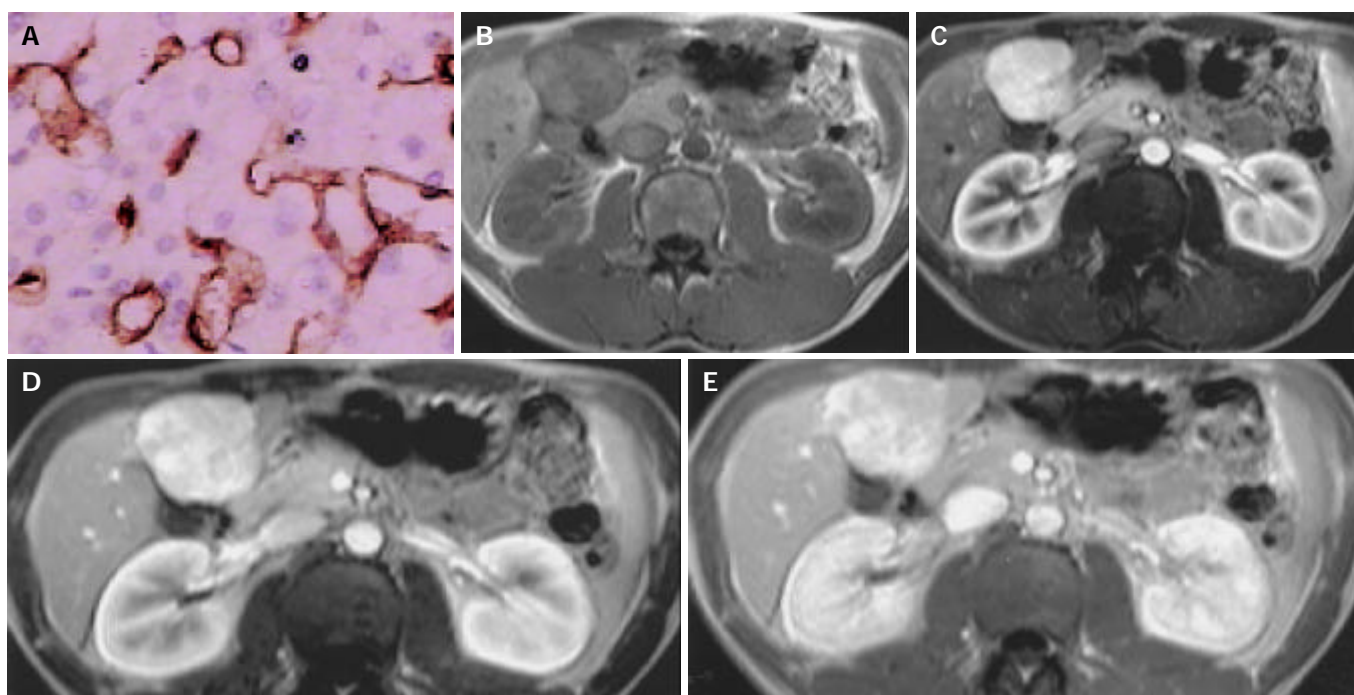


Figure 4 FNH in left inner lobar of liver. A: Microvessel density, stained by CD34 (Original magnification: $\times 200$); B: MR image, T1 weighted, nonenhanced, $CNR = -3.48$; C: MR image, arterial phase, $CNR = 15.43$; D: MR image, portal venous phase, $CNR = 5.81$; E: MR image, equilibrium phase, $CNR = 2.97$.

MVD of HCC among different pathological grades and tumor sizes

MVD of grades I-II was 29.9 ± 18.6 (mean \pm SD), which was much higher than those of grade III (22.2 ± 18.2 , $P < 0.01$) and grade IV (22.9 ± 19.0 , $P < 0.01$). There was no significant difference in MVD between small HCC (26.1 ± 15.3) and those HCC whose diameters were more than 3 cm (22.1 ± 15.8).

CNR of HCC and benign lesion in all the phases

CNRs of HCC and benign lesion in T1 weighted nonenhanced, arterial, portal venous and equilibrium phases are shown in

Table 2. There was significant difference among all the phases ($F = 9.761$, $P < 0.001$), but no significant difference among nonenhanced, portal venous and equilibrium phases ($P = 0.279$) or between HCC and benign lesion ($F = 0.380$, $P = 0.539$).

Correlation between MVD and CNRs

Forty-eight patients with 49 of the lesions underwent MRI examination before surgery, including 33 HCC (only one belonged to grade IV, and the others belonged to grade III and all the diameters were ≤ 3 cm) and 16 benign lesions. Pearson

Correlation coefficients among MVD and CNRs of HCC in arterial, portal venous and equilibrium phases were 0.409 ($P=0.018$), 0.264 ($P=0.138$) and 0.212 ($P=0.236$), respectively, while Pearson Correlation coefficients between MVD and CNRs of benign lesions in arterial, portal venous and equilibrium phases were 0.599 ($P=0.014$), 0.581 ($P=0.018$) and 0.540 ($P=0.031$), respectively.

Table 2 CNR of HCC and benign lesion (mean±SD)

	Nonenhanced	Arterial phase	Portal venous phase	Equilibrium phases
HCC (n=33)	-2.86±2.94	3.88±5.63	-1.43±8.39	-1.08±2.80
Benign lesion (n=16)	-2.91±2.79	2.12±9.08	-2.05±8.56	-0.92±6.59

Correlation between MVD and EIs

Pearson Correlation coefficients between MVD and EIs of the 33 specimens of HCC in arterial, portal venous and equilibrium phases were 0.155 ($P=0.389$), 0.072 ($P=0.692$) and -0.122 ($P=0.497$), respectively, while Pearson Correlation coefficients between MVD and EIs of the 16 specimens of benign lesions in arterial, portal venous and equilibrium phases were 0.077 ($P=0.776$), 0.180 ($P=0.506$) and -0.062 ($P=0.821$), respectively.

DISCUSSION

Utilization of tissue microarray technique in detecting nucleic acid and protein has recently made great progress in basic research of tumor. A large number of samples in one section of tissue microarray can be stained under the same pre-treatment condition, the same antibody titer and the same detection systems. And reproducibility of the staining reaction, as well as the speed and reliability of the interpretation, is improved, since all the samples are on the same slide^[7,8]. Then, quickly and efficiently scanning a great number of specimens with tissue microarray can reduce mistakes not only from sample selecting and statistical analysis but also from tumor heterogeneity. In MVD counting, utilization of tissue microarray can standardize sample areas and overcome manual deviation. In this research, tissue microarray technique, combined with immunohistochemistry, was used to study difference of MVD between malignant and benign hepatic lesions in order to further demonstrate some biological features of these lesions.

CD34, which is expressed in blood stem cells and neovessel endothelial cells, is the most distinctive marker for demonstrating vessel endothelial cells^[9,10], especially for demonstrating sinusoid-like vessels in tumor tissues^[11,12]. Angiogenesis is very common within normal and pathologic tissues and is regulated by many factors, such as hypoxia-inducible factor 1alpha (HIF-1 α), vascular endothelial growth factor (VEGF), human macrophage metalloelastase (HME), basic fibroblast growth factor (bFGF) and so on^[13-16]. Vessels, as an important part of tumor interstitial tissue, interact with tumor cells to construct microenvironment of tumor. Researches showed that angiogenesis plays an important role in tumor invasion^[17], MVD is a novel prognostic marker in patients after resection of small HCC^[11,18-20], and high expression of CD34-positive sinusoidal endothelial cells is a risk factor for HCC in patients with chronic liver diseases^[21]. Sun *et al.*^[18] reported that MVD level was not related to tumor size, capsule status, Edmondson-Steiner's grade, alpha-fetoprotein (AFP) level, associated cirrhosis, gamma-glutamyltransferase and serum HBsAg status. Yamamoto *et al.*^[22] demonstrated that sinusoidal capillarization occurring in well-differentiated HCC is related to dedifferentiation of parenchymal tumor cells, but not to tumor size. But some reports showed that tumor size, poor differentiation and portal invasion are significantly related to MVD^[11,23]. In this research,

MVD of HCC was significantly higher than that of cirrhosis, but there was no significant difference between those of HCC and of benign lesion, which probably means that microvessels play an important role not only in occurrence and development of HCC, but also in some other benign lesions, thus may be helpful to identify malignant lesions or precancerous lesions (for example, high-grade dysplastic nodule) from regenerative nodules or low-grade dysplastic nodules^[24,25]. MVD in grades I-II was higher than those in grade III and grade IV, suggesting that angiogenesis is more active during the beginning of hepatocarcinogenesis.

DSA and CTAP have been used for assessing angiogenesis of HCC^[6], but these examinations are all invasive and expensive with dangerousnesses of ionized radiation and allergy induced by iodine contrast material. Shimizu *et al.*^[26] used xenon-enhanced CT to quantitatively measure tissue blood flow in HCC, but xenon is a kind of scarce gas. Compared with DSA, CTAP and xenon-enhanced CT, MRI is uninvase, safe, rapid, and cheap. Gadolinium has a strong hydrogen-proton spin-lattice relaxation effect, which will increase the signal intensity of adjacent tissue on T1 weighted images. The MRI contrast agent, gadolinium-DTPA, does not penetrate cell membrane and only diffuses into vascular space and interstitial space, which may reveal that the signal intensity of tissue on enhanced T1 weighted image is correlated with the vascularity. There have been reports on correlation of dynamic contrast enhancement MRI with MVD in prostate cancer and in breast cancer^[27,28]. With development of fast scan technique, rapid MRI is available to image the whole liver during the arterial phase^[29]. In this research, CNR in arterial phase, regardless of malignant or benign lesions, was correlative with MVD. Since MVD of HCC is much higher than that of cirrhosis, arterial phase images of MRI could be a useful method to distinguish HCC from regenerative nodules. Some reports have confirmed this view^[30,31]. In this research, CNR of HCC in portal venous or equilibrium phase was not correlated with MVD. This phenomenon probably demonstrates that CNR is regulated by many factors besides MVD. Reports have shown that with small HCC increasing in size and becoming increasingly dedifferentiated, the number of portal tracts apparently decreases and intratumoral arteriole develops^[22,23]. Because of portal tracts' decreasing and intratumoral arterioles' developing, there was no unified blood supply in HCC nodules, which would not demonstrate unified relationship between MVD and CNR in portal venous or equilibrium phase. There was no change of blood supply in benign nodules, so unified relationship between MVD and CNR in portal venous or equilibrium phase was demonstrated. CNR in arterial phase is mostly regulated by MVD, while in portal venous or equilibrium phase, blood supply plays a more important role. This hypothesis should be tested by advanced research.

In conclusion, angiogenesis is secondary to occurrence and development of benign and malignant tumors. Since dynamic MRI could evaluate microvessel of lesions, it is a very useful method to demonstrate HCC.

REFERENCES

- 1 **El-Assal ON**, Yamanoi A, Soda Y, Yamaguchi M, Igarashi M, Yamamoto A, Nabika T, Nagasue N. Clinical significance of microvessel density and vascular endothelial growth factor expression in hepatocellular carcinoma and surrounding liver: possible involvement of vascular endothelial growth factor in the angiogenesis of cirrhotic liver. *Hepatology* 1998; **27**: 1554-1562
- 2 **Kallioniemi OP**, Wagner U, Kononen J, Sauter G. Tissue microarray technology for high-throughput molecular profiling of cancer. *Hum Mol Genet* 2001; **10**: 657-662
- 3 **Tomemori T**, Yamakado K, Nakatsuka A, Sakuma H, Matsumura K, Takeda K. Fast 3D dynamic MR imaging of the liver with MR SmartPrep: comparison with helical CT in de-

- etecting hypervascular hepatocellular carcinoma. *Clin Imaging* 2001; **25**: 355-361
- 4 **Shinozaki K**, Honda H, Yoshimitsu K, Taguchi K, Kuroiwa T, Irie H, Aibe H, Nishie A, Nakayama T, Shimada M, Masuda K. Optimal multi-phase three-dimensional fast imaging with steady-state free precession dynamic MRI and its clinical application to the diagnosis of hepatocellular carcinoma. *Radiat Med* 2002; **20**: 111-119
 - 5 **Noguchi Y**, Murakami T, Kim T, Hori M, Osuga K, Kawata S, Okada A, Sugiura T, Tomoda K, Narumi Y, Nakamura H. Detection of hypervascular hepatocellular carcinoma by dynamic magnetic resonance imaging with double-echo chemical shift in-phase and opposed-phase gradient echo technique: comparison with dynamic helical computed tomography imaging with double arterial phase. *J Comput Assist Tomogr* 2002; **26**: 981-987
 - 6 **Toyoda H**, Fukuda Y, Hayakawa T, Kumada T, Nakano S. Changes in blood supply in small hepatocellular carcinoma: correlation of angiographic images and immunohistochemical findings. *J Hepatol* 1997; **27**: 654-660
 - 7 **Bubendorf L**, Kononen J, Koivisto P, Schraml P, Moch H, Gasser TC, Willi N, Mihatsch MJ, Sauter G, Kallioniemi OP. Survey of gene amplifications during prostate cancer progression by high-throughout fluorescence *in situ* hybridization on tissue microarrays. *Cancer Res* 1999; **59**: 803-806
 - 8 **Richter J**, Wagner U, Kononen J, Fijan A, Bruderer J, Schmid U, Ackermann D, Maurer R, Alund G, Knönagel H, Rist M, Wilber K, Anabitarte M, Hering F, Hardmeier T, Schönsberger A, Flury R, Jager P, Fehr JL, Schraml P, Moch H, Mihatsch MJ, Gasser T, Källioniemi OP, Sauter G. High-throughput tissue microarray analysis of cyclin E gene amplification and overexpression in urinary bladder cancer. *Am J Pathol* 2000; **157**: 787-794
 - 9 **Kimura H**, Nakajima T, Kagawa K, Deguchi T, Kakusui M, Katagishi T, Okanou T, Kashima K, Ashihara T. Angiogenesis in hepatocellular carcinoma as evaluated by CD34 immunohistochemistry. *Liver* 1998; **18**: 14-19
 - 10 **Frachon S**, Gouysse G, Dumortier J, Couvelard A, Nejjar M, Mion F, Berger F, Paliard P, Boillot O, Scoazec JY. Endothelial cell marker expression in dysplastic lesions of the liver: an immunohistochemical study. *J Hepatol* 2001; **34**: 850-857
 - 11 **Tanigawa N**, Lu C, Mitsui T, Miura S. Quantitation of sinusoid-like vessels in hepatocellular carcinoma: its clinical and prognostic significance. *Hepatology* 1997; **26**: 1216-1223
 - 12 **Gottschalk-Sabag S**, Ron N, Glick T. Use of CD34 and factor VIII to diagnose hepatocellular carcinoma on fine needle aspirates. *Acta Cytol* 1998; **42**: 691-696
 - 13 **Ravi R**, Mookerjee B, Bhujwala ZM, Sutter CH, Artemov D, Zeng Q, Dillehay LE, Madan A, Semenza GL, Bedi A. Regulation of tumor angiogenesis by p53-induced degradation of hypoxia-inducible factor 1alpha. *Genes Dev* 2000; **14**: 34-44
 - 14 **Gorrin-Rivas MJ**, Arie S, Mori A, Takeda Y, Mizumoto M, Furutani M, Imamura M. Implications of human macrophage metalloelastase and vascular endothelial growth factor gene expression in angiogenesis of hepatocellular carcinoma. *Ann Surg* 2000; **231**: 67-73
 - 15 **Yoshiji H**, Kuriyama S, Yoshii J, Ikenaka Y, Noguchi R, Hicklin DJ, Huber J, Nakatani T, Tsujinoue H, Yanase K, Imazu H, Fukui H. Synergistic effect of basic fibroblast growth factor and vascular endothelial growth factor in murine hepatocellular carcinoma. *Hepatology* 2002; **35**: 834-842
 - 16 **Park YN**, Kim YB, Yang KM, Park C. Increased expression of vascular endothelial growth factor and angiogenesis in the early stage of multistep hepatocarcinogenesis. *Arch Pathol Lab Med* 2000; **124**: 1061-1065
 - 17 **Ker CG**, Chen HY, Juan CC, Lo HW, Shen YY, Chen JS, Lee KT, Sheen PC. Role of angiogenesis in hepatitis and hepatocellular carcinoma. *Hepatogastroenterology* 1999; **46**: 646-650
 - 18 **Sun HC**, Tang ZY, Li XM, Zhou YN, Sun BR, Ma ZC. Microvessel density of hepatocellular carcinoma: its relationship with prognosis. *J Cancer Res Clin Oncol* 1999; **125**: 419-426
 - 19 **Salizzoni M**, Romagnoli R, Lupo F, David E, Mirabella S, Cerutti E, Ottobrelli A. Microscopic vascular invasion detected by anti-CD34 immunohistochemistry as a predictor of recurrence of hepatocellular carcinoma after liver transplantation. *Transplantation* 2003; **76**: 844-848
 - 20 **Poon RT**, Ng IO, Lau C, Yu WC, Yang ZF, Fan ST, Wong J. Tumor microvessel density as a predictor of recurrence after resection of hepatocellular carcinoma: a prospective study. *J Clin Oncol* 2002; **20**: 1775-1785
 - 21 **Ohmori S**, Shiraki K, Sugimoto K, Sakai T, Fujikawa K, Wagayama H, Takase K, Nakano T. High expression of CD34-positive sinusoidal endothelial cells is a risk factor for hepatocellular carcinoma in patients with HCV-associated chronic liver diseases. *Hum Pathol* 2001; **32**: 1363-1370
 - 22 **Yamamoto T**, Hirohashi K, Kaneda K, Ikebe T, Mikami S, Uenishi T, Kanazawa A, Takemura S, Shuto T, Tanaka H, Kubo S, Sakurai M, Kinoshita H. Relationship of the microvascular type to the tumor size, arterIALIZATION and dedifferentiation of human hepatocellular carcinoma. *Jap J Cancer Res* 2001; **92**: 1207-1213
 - 23 **Nakashima Y**, Nakashima O, Hsia CC, Kojiro M, Tabor E. Vascularization of small hepatocellular carcinomas: correlation with differentiation. *Liver* 1999; **19**: 12-18
 - 24 **Roncalli M**, Roz E, Coggi G, Di Rocco MG, Bossi P, Minola E, Gambacorta M, Borzio M. The vascular profile of regenerative and dysplastic nodules of the cirrhotic liver: implications for diagnosis and classification. *Hepatology* 1999; **30**: 1174-1178
 - 25 **de Boer WB**, Segal A, Frost FA, Sterrett GF. Can CD34 discriminate between benign and malignant hepatocytic lesions in fine-needle aspirates and thin core biopsies? *Cancer* 2000; **90**: 273-278
 - 26 **Shimizu J**, Oka H, Dono K, Sakon M, Takamura M, Murakami T, Hayashi S, Nagano H, Nakamori S, Umeshita K, Sase S, Gotoh M, Wakasa K, Nakamura H, Monden M. Noninvasive quantitative measurement of tissue blood flow in hepatocellular carcinoma using xenon-enhanced computed tomography. *Dig Dis Sci* 2003; **48**: 1510-1516
 - 27 **Schlemmer HP**, Merkle J, Grobholz R, Jaeger T, Michel MS, Werner A, Rabe J, van Kaick G. Can pre-operative contrast-enhanced dynamic MR imaging for prostate cancer predict microvessel density in prostatectomy specimens? *Eur Radiol* 2004; **14**: 309-317
 - 28 **Su MY**, Cheung YC, Fruehauf JP, Yu H, Nalcioğlu O, Mechetner E, Kyshtoobayeva A, Chen SC, Hsueh S, McLaren CE, Wan YL. Correlation of dynamic contrast enhancement MRI parameters with microvessel density and VEGF for assessment of angiogenesis in breast cancer. *J Magn Reson Imaging* 2003; **18**: 467-477
 - 29 **Van Beers BE**, Materne R, Lacrosse M, Jamart J, Smith AM, Horsmans Y, Gigot JF, Gilon R, Pringot J. MR imaging of hypervascular liver tumors: timing optimization during the arterial phase. *J Magn Reson Imaging* 1999; **9**: 562-567
 - 30 **Yoshimitsu K**, Honda H, Jimi M, Kuroiwa T, Irie H, Aibe H, Shinozaki K, Asayama Y, Shimada M, Masuda K. Correlation of three-dimensional gradient echo dynamic MR imaging with CT during hepatic arteriography in patients with hypervascular hepatocellular carcinomas: preliminary clinical experience. *J Magn Reson Imaging* 2001; **13**: 258-262
 - 31 **Noguchi Y**, Murakami T, Kim T, Hori M, Osuga K, Kawata S, Kumano S, Okada A, Sugiura T, Nakamura H. Detection of hepatocellular carcinoma: comparison of dynamic MR imaging with dynamic double arterial phase helical CT. *Am J Roentgenol* 2003; **180**: 455-460